The University of Osaka
Institutional Knowledge Archive

Title	Efficient focusing of hard x rays to 25 nm by a total reflection mirror
Author(s)	Mimura, Hidekazu; Yumoto, Hirokatsu; Matsuyama, Satoshi et al.
Citation	Applied Physics Letters. 2007, 90(5), p. 051903
Version Type	VoR
URL	https://hdl.handle.net/11094/86972
rights	This article may be downloaded for personal use only. Any other use requires prior permission of the author and AIP Publishing. This article appeared in Appl. Phys. Lett. 90(5), 051903 (2007) and may be found at https://doi.org/10.1063/1.2436469.
Note	

The University of Osaka Institutional Knowledge Archive : OUKA

https://ir.library.osaka-u.ac.jp/

The University of Osaka

AIP Applied Physics Letters

Efficient focusing of hard x rays to 25 nm by a total reflection mirror

Hidekazu Mimura, Hirokatsu Yumoto, Satoshi Matsuyama, Yasuhisa Sano, Kazuya Yamamura, Yuzo Mori, Makina Yabashi, Yoshinori Nishino, Kenji Tamasaku, Tetsuya Ishikawa, and Kazuto Yamauchi

Citation: Applied Physics Letters **90**, 051903 (2007); doi: 10.1063/1.2436469
View online: http://dx.doi.org/10.1063/1.2436469
View Table of Contents: http://scitation.aip.org/content/aip/journal/apl/90/5?ver=pdfcov
Published by the AIP Publishing

Articles you may be interested in

Kirkpatrick-Baez type x-ray focusing mirror fabricated by the bent-polishing method
Rev. Sci. Instrum. **76**, 093708 (2005); 10.1063/1.2052595

Diffraction-limited two-dimensional hard-x-ray focusing at the 100 nm level using a Kirkpatrick-Baez mirror arrangement
Rev. Sci. Instrum. **76**, 083114 (2005); 10.1063/1.2005427

X-Ray Focusing Mirror Fabricated With Bent-Polishing Method
AIP Conf. Proc. **705**, 760 (2004); 10.1063/1.1757907

Two-dimensional X-ray focusing by crystal bender and mirrors
AIP Conf. Proc. **705**, 720 (2004); 10.1063/1.1757897

The design and performance of an x-ray micro-focusing system using differentially deposited elliptical mirrors at the National Synchrotron Light Source
Rev. Sci. Instrum. **73**, 3464 (2002); 10.1063/1.1505656

Reuse of AIP Publishing content is subject to the terms at: https://publishing.aip.org/authors/rights-and-permissions. Download to IP: 133.1.116.104 On: Mon, 09 May 2016 06:18:01

Efficient focusing of hard x rays to 25 nm by a total reflection mirror

Hidekazu Mimura,[a] Hirokatsu Yumoto, Satoshi Matsuyama, and Yasuhisa Sano
Department of Precision Science and Technology, Graduate School of Engineering, Osaka University, 2-1 Yamada-oka, Suita, Osaka 565-0871, Japan

Kazuya Yamamura and Yuzo Mori
Center for Ultra Precision Science and Technology, Graduate School of Engineering, Osaka University, 2-1 Yamada-oka, Suita, Osaka 565-0871, Japan

Makina Yabashi
SPring-8/Japan Synchrotron Radiation Research Institute (JASRI), 1-1-1, Kouto, Sayo-cho, Sayo-gun, Hyogo 679-5198, Japan

Yoshinori Nishino, Kenji Tamasaku, and Tetsuya Ishikawa
SPring-8/RIKEN, 1-1-1, Kouto, Sayo-cho, Sayo-gun, Hyogo 679-5198, Japan

Kazuto Yamauchi
Department of Precision Science and Technology, Graduate School of Engineering, Osaka University, 2-1 Yamada-oka, Suita, Osaka 565-0871, Japan

(Received 4 August 2006; accepted 2 January 2007; published online 29 January 2007)

Nanofocused x rays are indispensable because they can provide high spatial resolution and high sensitivity for x-ray nanoscopy/spectroscopy. A focusing system using total reflection mirrors is one of the most promising methods for producing nanofocused x rays due to its high efficiency and energy-tunable focusing. The authors have developed a fabrication system for hard x-ray mirrors by developing elastic emission machining, microstitching interferometry, and relative angle determinable stitching interferometry. By using an ultraprecisely figured mirror, they realized hard x-ray line focusing with a beam width of 25 nm at 15 keV. The focusing test was performed at the 1-km-long beamline of SPring-8. © *2007 American Institute of Physics*. [DOI: 10.1063/1.2436469]

Advances in synchrotron radiation facilities have been accelerating the progress of various x-ray analysis methods. Focused hard x-ray beams are employed in various scanning-type microscopes to give precise spatial information for signals such as fluorescence, absorption, and diffraction x rays. There are many types of hard x-ray focusing devices that utilize reflection,[1–3] refraction,[4] and diffraction[5,6] optics. In the past decade, rapid advances in microfabrication technology, high-precision surface finishing, crystal growth, controlled-layer deposition, and precision metrology have led to the realization of hard x-ray focusing to nanometer dimensions. Most hard x-ray focusing methods have the ability to focus hard x rays down to the 100 nm level.[1–6]

The inherently nondispersive nature of total-external-reflection mirrors for x-ray nanofocusing is one of their most attractive features from the viewpoint of spectroscopic applications that usually require broad bandpass or energy tunability. Kirkpatrick-Baez (KB) mirrors are being developed for this purpose. These mirrors are based on a classical method that utilizes two concave mirrors at a glancing angle to collect and focus x rays in both vertical and horizontal planes. Recently, construction of an x-ray free-electron laser has been planned as a next-generation x-ray source.[7] Total reflection mirrors are considered to be the best focusing optics for such an x-ray source because of their high efficiency and radiation hardness.

The physical limit for the spot size to which hard x rays can be focused using total-reflection-based optics has already been discussed and estimated.[8,9] An ultimate diffraction-limited size can easily be calculated using the formula λ/NA for the case of a rectangular aperture, where NA is the numerical aperture and λ is the wavelength of the x rays. The NA is fundamentally limited by the critical angle θ_c of the external total reflection. In the hard x-ray region, it is well known that θ_c (rad) can be expressed as $1.6\times10^{-2}\,\lambda\,\rho^{1/2}$, where ρ (g/cm^3) is the density of the mirror material and λ (nm) is the x-ray wavelength. Performing this calculation gives a size that is slightly smaller than 10 nm, when available heavy materials such as platinum, are employed for the surface material.

However, the working distance needs to be long for practical applications, the mirror length is also limited and two identical mirrors are required in the KB arrangement. For this reason the smallest practical beam size is considered to be around 20 nm. To obtain a smaller size using reflective optics, multilayer coating is necessary on mirror surfaces to realize higher-NA design.

In this letter, we report the fabrication of an ultraprecise x-ray mirror for hard x-ray focusing and realization of the diffraction-limited line focusing that results in a beam width of approximately 25 nm. The mirror was fabricated using a computer-controlled surface figuring system, in which elastic emission machining (EEM) was employed as the machining method and microstitching interferometry (MSI) and relative angle determinable stitching interferometry (RADSI) were used as surface figure measurement methods. A surface figure accuracy of 2 nm (peak to valley) was achieved. The one-dimensional hard x-ray focusing test was performed at the 1-km-long beamline (BL29XUL) of SPring-8. The measured beam size is in good agreement with the theoretical one, that is, the diffraction-limited size.

[a]Electronic mail: mimura@prec.eng.osaka-u.ac.jp

Reuse of AIP Publishing content is subject to the terms at: https://publishing.aip.org/authors/rights-and-permissions. Download to IP: 133.1.116.104 On: Mon, 09 May 2016 06:18:01

 © 2007 American Institute of Physics

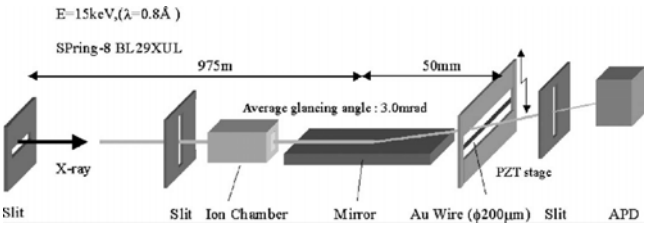

FIG. 1. Schematic illustration of experimental setup for evaluating x-ray nanofocusing mirror. The intensity profile on the focal plane is measured by the wire scanning method.

An elliptic function was used to design the surface profile of the mirror. The designed surface profile has the partial profile of an elliptic function, one focal point of which is at the incident slit, which is the x-ray source, while the other focal point is at the point where the x rays are collected. By employing a heavy metal surface as the reflective surface, an incident ray can be totally reflected even at large glancing angles. In this study, the silicon substrate surface was coated with platinum. The optical design was determined by taking into account the properties of the 1-km-long beamline of SPring-8.[10,11] Figure 1 shows a schematic illustration of the optical design in the experiment. The distance between the incident slit and the mirror was 975 m. The mirror length was 45 mm. The maximum incident angle was 4.2 mrad, which is approximately equal to the critical angle of the platinum surface at 18 keV. When the incident angle is 4.2 mrad the x-ray reflectivity is approximately 70% at 15 keV. In this study, to obtain high reflectivity at the entire mirror area, an x-ray energy of 15 keV was selected. The average incident angle was approximately 3 mrad. The focal length was set to be 50 mm.

Figure 2(a) shows the elliptical profile that was designed for this experiment. The estimated focal size, defined as the full width at half maximum in the intensity profile, is 25 nm at 15 keV for diffraction-limited conditions. The relationship between the figure error characteristics and the focusing properties of the mirror was investigated previously using a wave-optical simulator and is described in previous study..[12] In this case, in order to realize the ideal beam focal size, the figure accuracy needed to be at least 3 nm (peak to valley) at spatial wavelength ranges larger than 10 mm. In addition, the high-frequency figure error and the surface roughness should be less than 0.2 nm (rms) to realize ideal focusing efficiency.

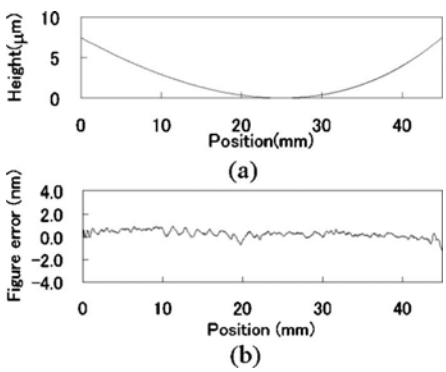

FIG. 2. Elliptical profile (a) and figure error profile (b) of the fabricated focusing mirror. A figure accuracy of 0.15 nm (rms) was achieved. This surface is produced by EEM.

The silicon substrate surface shape of the tested x-ray mirror was fabricated using EEM figuring at the required accuracy.[13–16] There are two types of EEM; the difference between them lies in the EEM head, which is the device for supplying particles to the processed surfaces. One method is called nozzle-head-type EEM, and it is employed for computer-controlled figuring. The other method is called rotary-spherical-head-type EEM, and it is used for surface supersmoothing.[17] By combining these two methods, it is possible to produce surfaces that have a previously unobtainable accuracy and smoothness, namely, a figure accuracy and a roughness of 0.15 nm (rms).

Metrology plays an important role in figuring because computer-controlled figuring is performed using measured surface profiles.[18–20] We developed MSI, which uses microscopic and large-area phase-shifting interferometers, to measure the surface profiles of x-ray mirrors with a reproducibility of smaller than 1 nm (peak to valley) and with a spatial resolution of approximately 20 μm.[19] RADSI was developed to measure strongly curved profiles to the required accuracy.[12] In this stitching system, several partial profiles that span the entire area are measured using a Fizeau interferometer. These profiles are then stitched together to generate a profile of the entire surface. The stitching method employed uses stitching angles that are determined, not by the conventional method, which utilizes the overlapping areas of adjacent profiles, but by a new method that utilizes the tilt angles of the mirror measured when the profiles are acquired.

The key point for fabricating designed elliptically curved surfaces is improvement of the metrology, because the measurement accuracy determines the final figure accuracy of the fabricated mirror. The designed surface profile is steeply curved profile. In RADSI,[12] the measurable area is smaller than that obtained for our previously x-ray mirror. In this study, before fabricating the mirror, the RADSI system was improved by recoding the surface-profile stitching program and stabilizing the measurement environment, in particular, the vibration. By combining MSI and improved RADSI, it was possible to acquire surface profiles to the required degree of accuracy.

Figure 2(b) shows the surface figure error profile obtained after platinum deposition. Film thickness is approximately 40 nm. A figure accuracy of 0.15 nm (rms) was achieved. Platinum deposition was finally performed using an electron-beam evaporation system. In this system, the mirror surface is passed over a small aperture located approximately 400 mm above the evaporation source, while the source power is controlled by a feedback system to maintain a constant deposition rate. The surface profiles before and after platinum coating were compared and found to be in good agreement at the subnanometer level.

The line-focusing test was performed at the 1-km-long beamline (BL29XUL) of SPring-8, which produces hard x rays of sufficiently high coherence for nanofocusing.[10,11] Monochromatic x rays at 15 keV were produced with a cryogenically cooled double-crystal silicon (111) monochromator and guided to an experimental hutch located 1 km from the monochromator. Wire scanning was used for measuring the intensity profiles. A piezoactuated translation stage enabled wire scanning to be performed at 1 nm increments. A gold wire having a diameter of 200 μm was placed at the designed focal position. An avalanche photodiode detector placed behind the wire was used for measuring the beam

Reuse of AIP Publishing content is subject to the terms at: https://publishing.aip.org/authors/rights-and-permissions. Download to IP: 133.1.116.104 On: Mon, 09 May 2016 06:18:01

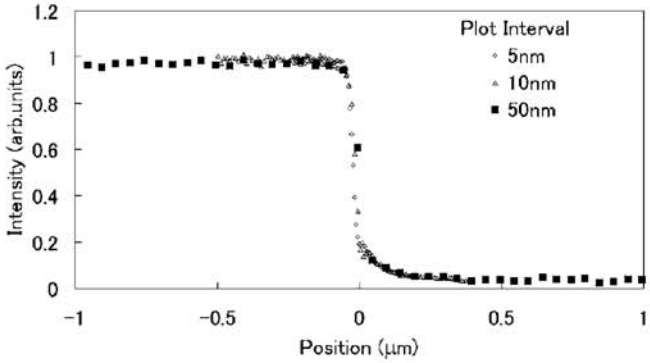

FIG. 3. Relationship between wire position and beam intensity measured by an x-ray photon detector located behind the wire. Plot interval is from 5 to 50 nm.

intensity during wire scanning. All alignment parameters, except for the glancing angle, were preadjusted when the mirror was placed into position. Precise adjustment of the glancing angles was performed while monitoring the intensity profile until optimum focusing was achieved.

Figure 3 shows the relationship between the measured intensity using the avalanche photodiode and the wire position. In order to investigate focusing efficiency, which is defined as the ratio of the number of photons in the focused beam to the number of photons reflected from the mirror surfaces, relatively long distance wire scanning using a plot interval of 50 nm was carried out. When the wire did not obscure the beam completely, the detected x-ray intensity was almost equal to unity, which is the theoretically ideal value when the ideal reflectivity and the effect of absorption in air are taken into account. The steep decline in the graph indicates that 90% of the photons are reflected x rays collected in a focused region smaller than 100 nm. Figure 4 shows the intensity profile of the focused beam calculated by differentiating the curve using a data interval of 5 nm, together with the ideal profiles simulated using wave-optical theory. The focal size, defined as the full width at half maximum of the intensity profile, is 25 nm. Figure 4 shows raw data, which were affected by the transmission and reflection effects of the passage of the x ray through the wire. However, the measured profile in Fig. 4 agrees reasonably well with the ideal profile. This fact indicates that both beam profile measurement and mirror figure quality are at a satisfactory level for 25 nm focusing in the hard x-ray region.

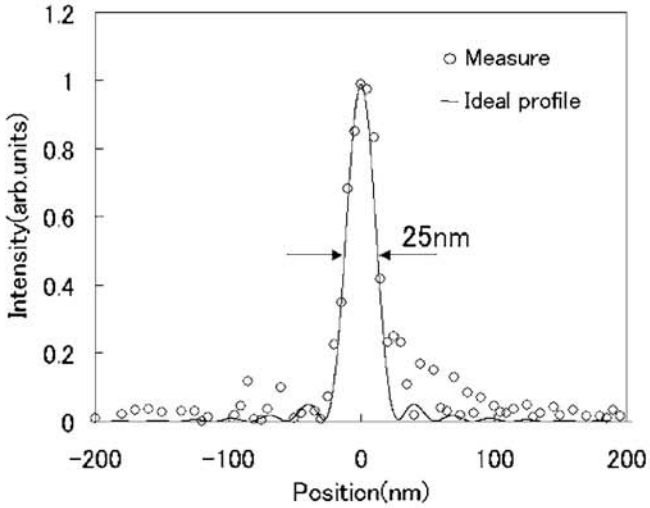

FIG. 4. Intensity distribution profile of focused beam. This profile was obtained by differentiating the curve shown in Fig. 3 using a 5 nm interval.

In conclusion, we have realized hard x-ray line focusing having a focal size of approximately 25 nm. By coupling one more mirror having a relatively long focal length and working distance, two-dimensional focusing producing a beam size of less than 30 nm is possible. In addition, it is possible to realize low background noise around the main peak, which is very important for achieving good visibility in x-ray microscopy analysis.

This research was supported by a Grant-in-Aid for Specially Promoted Research 18002009, 2006 and 21st Century COE Research, Center for Atomistic Fabrication Technology, 2006 from the Ministry of Education, Sports, Culture, Science and Technology, Japan. The use of BL29XU of the SPring-8 was supported by RIKEN.

[1]W. Liu, G. E. Ice, J. Z. Tischler, A. Khounsary, C. Liu, L. Assoufid, and A. T. Macrander, Rev. Sci. Instrum. **76**, 113701 (2005).
[2]H. Mimura, S. Matsuyama, H. Yumoto, K. Yamamura, Y. Sano, M. Shibahara, K. Endo, Y. Mori, Y. Nishino, K. Tamasaku, M. Yabashi, T. Ishikawa, and K. Yamauchi, Jpn. J. Appl. Phys., Part 2 **44**, L539 (2005).
[3]O. Hignette, P. Cloetens, G. Rostaing, P. Bernard, and C. Morawe, Rev. Sci. Instrum. **76**, 063709 (2005).
[4]C. G. Schroer, M. Kuhlmann, T. F. Günzler, B. Lengeler, M. Richwin, B. Griesebock, D. Lützenkirchen-Hecht, R. Frahm, E. Ziegler, A. Mashayekhi, D. R. Haeffner, J.-D. Grunwaldt, and A. Baiker, Appl. Phys. Lett. **82**, 3360 (2003).
[5]H. Takano, Y. Suzuki, and A. Takeuchi, Jpn. J. Appl. Phys., Part 2 **42**, L132 (2003).
[6]H. C. Kang, J. Maser, G. B. Stephenson, C. Liu, R. Conley, A. T. Macrander, and S. Vogt, Phys. Rev. Lett. **96**, 127401 (2006).
[7]T. Shintake, T. Tanaka, T. Hara, K. Togawa, T. Inagaki, Y. J. Kim, T. Ishikawa, H. Kitamura, H. Baba, H. Matsumoto, S. Takeda, M. Yoshida, and Y. Takasu, Nucl. Instrum. Methods Phys. Res. A **507**, 382 (2003).
[8]P. Kirkpatrick and A. V. Baez, J. Opt. Soc. Am. **38**, 766 (1948).
[9]Y. Suzuki, Jpn. J. Appl. Phys., Part 1 **43**, 7311 (2004).
[10]T. Ishikawa, K. Tamasaku, M. Yabashi, S. Goto, Y. Tanaka, H. Yamazaki, K. Takeshita, H. Kimura, H. Ohashi, T. Matsushita, and T. Ohata, Proc. SPIE **4115**, 1 (2001).
[11]K. Tamasaku, Y. Tanaka, M. Yabashi, H. Yamazaki, N. Kawamura, M. Suzuki, and T. Ishikawa, Nucl. Instrum. Methods Phys. Res. A **467–468**, 686 (2001).
[12]H. Mimura, H. Yumoto, S. Matsuyama, K. Yamamura, Y. Sano, K. Ueno, K. Endo, Y. Mori, M. Yabashi, Y. Nishino, K. Tamasaku, M. Yabashi, T. Ishikawa, and K. Yamauchi, Rev. Sci. Instrum. **76**, 045102 (2005).
[13]K. Yamauchi, K. Yamamura, H. Mimura, Y. Sano, A. Saito, K. Endo, A. Souvorov, M. Yabashi, K. Tamasaku, T. Ishikawa, and Y. Mori, Jpn. J. Appl. Phys., Part 1 **42**, 7129 (2003).
[14]K. Yamauchi, K. Yamamura, H. Mimura, Y. Sano, A. Saito, A. Souvorov, M. Yabashi, K. Tamasaku, T. Ishikawa, and Y. Mori, J. Synchrotron Radiat. **9**, 313 (2002).
[15]K. Yamauchi, H. Mimura, K. Inagaki, and Y. Mori, Rev. Sci. Instrum. **73**, 4028 (2002).
[16]H. Mimura, K. Yamauchi, K. Yamamura, A. Kubota, S. Matsuyama, Y. Sano, K. Ueno, K. Endo, Y. Nishino, K. Tamasaku, M. Yabashi, T. Ishikawa, and Y. Mori, J. Synchrotron Radiat. **11**, 343 (2004).
[17]Y. Mori, K. Yamauchi, K. Yamamura, H. Mimura, A. Saito, H. Kishimoto, Y. Sekito, M. Kanaoka, A. Souvorov, M. Yabashi, T. Kenji, and T. Ishikawa, Proc. SPIE **4501**, 30 (2001).
[18]P. Z. Takacs, E. L. Church, C. J. Bresloff, and L. Assoufid, Appl. Opt. **38**, 5468 (1999).
[19]K. Yamauchi, K. Yamamura, H. Mimura, Y. Sano, A. Saito, K. Ueno, K. Endo, A. Souvorov, M. Yabashi, K. Tamasaku, T. Ishikawa, and Y. Mori, Rev. Sci. Instrum. **74**, 2894 (2003).
[20]H. Yumoto, H. Mimura, S. Matsuyama, K. Yamamura, Y. Sano, K. Ueno, K. Endo, Y. Mori, Y. Nishino, M. Yabashi, K. Tamasaku, T. Ishikawa, and K. Yamauchi, Rev. Sci. Instrum. **76**, 063708 (2005).

Reuse of AIP Publishing content is subject to the terms at: https://publishing.aip.org/authors/rights-and-permissions. Download to IP: 133.1.116.104 On: Mon, 09 May 2016 06:18:01